

PROCEEDINGS OF SPIE

SPIDigitalLibrary.org/conference-proceedings-of-spie

Femtosecond laser-written double line waveguides in germanate and tellurite glasses

Diego S. da Silva, Niklaus U. Wetter, Wagner de Rossi, Ricardo E. Samad, Luciana R. P. Kassab

Diego S. da Silva, Niklaus U. Wetter, Wagner de Rossi, Ricardo E. Samad, Luciana R. P. Kassab, "Femtosecond laser-written double line waveguides in germanate and tellurite glasses," Proc. SPIE 10519, Laser Applications in Microelectronic and Optoelectronic Manufacturing (LAMOM) XXIII, 105191B (16 February 2018); doi: 10.1117/12.2291223

SPIE.

Event: SPIE LASE, 2018, San Francisco, California, United States

Femtosecond Laser-Written Double Line Waveguides in Germanate and Tellurite glasses

Diego S. da Silva^a, Niklaus, U. Wetter^{*a}, Wagner de Rossi^a, Ricardo E. Samad^a, Luciana R. P. Kassab^b

^aCentro de Lasers e Aplicações. Instituto de Pesquisas Energéticas e Nucleares – IPEN-CNEN/SP. 2242 A. Prof. Lineu Prestes, São Paulo, Brazil; ^bFaculdade de Tecnologia de São Paulo, CEETEPS, 01124-060, São Paulo, Brazil.

ABSTRACT

The authors report the fabrication and characterization of passive waveguides in $\text{GeO}_2\text{-PbO}$ and $\text{TeO}_2\text{-ZnO}$ glasses written with a femtosecond laser delivering pulses with $3\mu\text{J}$, $30\mu\text{J}$ and 80fs at 4kHz repetition rate. Permanent refractive index change at the focus of the laser beam was obtained and waveguides were formed by two closely spaced laser written lines, where the light guiding occurs between them. The refractive index change at 632 nm is around 10^{-4} . The value of the propagation losses was around 2.0 dB/cm . The output mode profiles indicate multimodal guiding behavior. Raman measurements show structural modification of the glassy network. The results show that these materials are potential candidates for passive waveguides applications as low-loss optical components.

Keywords: double line waveguide, germanate, tellurite, femtosecond laser writing.

1. INTRODUCTION

Direct femtosecond (fs) laser writing of photonic components and circuits is currently a widely studied application in the area of processing transparent dielectrics¹⁻⁴. The capacity to modify the internal structure and the refractive index of optical glasses and other dielectrics via nonlinear absorption mechanisms is generally pointed out as the responsible phenomena involved, but its mechanisms are still not completely explained and are an ongoing research topic for many kind of materials. Depending on the material properties, as well as on the characteristics of the laser used for inscribing, two types of waveguides can be obtained: the first type consists of a single line, where the modification of the material causes a refractive index increase, leading to light confinement⁵. The second type consists of stress-induced positive refractive index changes in the region adjacent to the writing⁶, or negative refractive index changes in the laser focal region⁷. In the latter case, the light is guided between two or more written lines. Single line waveguides have the advantage of simpler and faster processing and have also been demonstrated in a variety of glasses including fused silica, borosilicate², chalcogenides³ and BK7⁴. Double line waveguides have been demonstrated in a number of hosts, including crystals^{6, 8-12}. This latter type of writing was the methodology used in this work after previous tests with both types of writing.

Heavy metal oxide glasses, like germanates and tellurites, are interesting materials for photonic applications due to properties such as their high linear refractive index (~ 2) that is responsible for a high nonlinear refractive index, their extensive transmission window from visible to near infrared, and a lower cutoff phonon energy ($< 700\text{ cm}^{-1}$) when compared to silicate, borate, and phosphate glasses. Previously we reported on the fabrication and characterization of active waveguides in $\text{GeO}_2\text{-PbO-Ga}_2\text{O}_3$ glass samples doped with Er^{3+} , written by a femtosecond laser delivering pulses of 80 fs duration at 1 kHz repetition rate. Single line waveguides were formed under different laser pulse energies and scan velocities, and the passive and active optical properties of the waveguides were investigated¹³.

This work presents, to the best of our knowledge, the first demonstration of waveguiding in germanate and tellurite glasses by double line writing by fs laser pulses.

*nuwetter@ipen.br; phone +55 11 3133 9359; www.ipen.br

2. EXPERIMENTAL

2.1 Preparation of glasses

High purity starting oxide powers (99.999%) were used in a conventional melting and quenching method, where the compounds were fully mixed in platinum (TeO_2 - ZnO) or aluminum (GeO_2 - PbO) crucibles, melted, and then poured into pre-heated brass molds in air, to avoid internal stress. The temperature and time duration for melting and annealing are presented in table 1 for each glass composition. After cooling, the samples were polished to acquire optical quality. Transparent and homogeneous glasses were produced.

Table 1. Parameters of the fabrication of the bulk glasses.

Glass	Composition (wt %)	Melting/ annealing temperature ($^{\circ}\text{C}$)	Melting/ annealing time (min)
TeO_2 - ZnO	TeO_2 : 85.0 ZnO : 15.0	800/325	20/120
GeO_2 - PbO	GeO_2 : 40.3 PbO : 59.7	1200/420	60/60

2.2 Waveguide writing:

The femtosecond laser setup consists of a Ti:Sapphire laser system operating at $\lambda = 800$ nm, able to deliver up to $800 \mu\text{J}$ of energy in a pulse with duration ranging from 25 to 200 fs, in a 4 kHz repetition rate pulse train (Femtopower Compact Pro HR/HP, from Femtolasers). Sample translation stages with 300 nm precision were controlled via an integrated CadCam system. The parameters used for writing the waveguides are shown in table 2. Several pairs of closely spaced, parallel waveguides were written using a $20\times$ objective lens with $\text{N.A} = 0.4$, focal length = 10 mm and depth of focus = $200 \mu\text{m}$, separated by a distance of $10 \mu\text{m}$, using laser energies of $3 \mu\text{J}$ and $30 \mu\text{J}$. The waveguides were written 0.7 mm beneath the sample's surface. After the waveguide writing, the glasses were re-polished at the input and output facets, which were damaged during the femtosecond writing process. The final length of the obtained waveguides was 1.0 cm.

Table 2. Parameters used in the writing process

Writing speed (mm/min)	1.0
Laser spot size (μm)	5.0
Pulse duration (fs)	80
Wavelength (nm)	800
Polarization in writing direction	parallel
Repetition rate (kHz)	4
Depth of focus (μm)	200

2.3 Materials and Waveguide Characterization:

Absorbance measurements at the laser focus were obtained to analyze how the transparency of the material is affected in this region using a spectrometer (Cary 5000). Optical transmission microscopy was used to capture the images of the laser written structures. A CCD camera was used to analyze how the laser processing affects the surface of the glasses. Figure 1 shows the setup used to determine the near field profile (using a CCD camera), optical losses (using a

Powermeter) and beam quality factor M^2 (using a measurement system formed by a CMOS controlled by a LabVIEWTM program) of a coupled HeNe beam. The optical losses were determined using equation 1, where P_2 represents the output power measured for a sample of length Z_2 , and P_1 the output power of a sample with reduced length Z_1 ¹⁴,

$$\text{Optical losses} = -\frac{10 \log\left(\frac{P_2}{P_1}\right)}{Z_2 - Z_1} \quad (1)$$

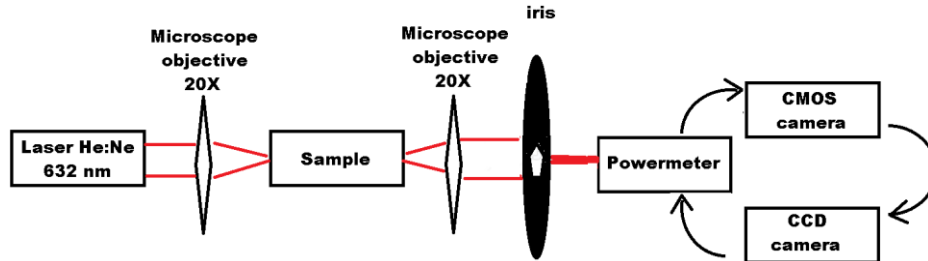


Figure 1. Basic schematic diagram used to determine the near field profile, optical losses and M^2 factor.

The refractive index contrast of the regions in the middle of the written lines and between two written lines was estimated by measuring the output signal of the waveguide at $1/e^2$ width, at a distance of several centimeters, and the numerical aperture (N.A) of the waveguides was calculated from the ratio between the distance and the mode radius. The refractive index change could be estimated by the measured N.A. of the waveguides, as described in ref¹⁵ by the basic equation 2, where n_1 and n_2 represent the refractive index of the core and the cladding, respectively. Raman spectroscopic measurements were made in the focal region of the writing and in the bulk glass using a confocal Raman Microscope (WITEC, model: Alpha300) at $\lambda = 532$ nm, power of 45 mW, wavenumber within the range of 0 to 3793 cm^{-1} , a $50\times$ objective and resolution of $0.464 \text{ }\mu\text{m}$.

$$N.A. = \sqrt{n_1^2 - n_2^2} \approx \sqrt{2n_2\Delta n} \quad (2)$$

3. RESULTS AND DISCUSSIONS

Figure 2 shows the absorption spectra of the TeO_2 -ZnO and GeO_2 -PbO glasses taken from the bulk and also from the waveguides written by $30 \text{ }\mu\text{J}$ pulses. The spectra for the waveguides processed with lower energy pulse ($3 \text{ }\mu\text{J}$) is not shown because there were no measurable differences between them and the bulk spectra. Comparing the results we observe a small change in the transmittance window, mainly for the GeO_2 -PbO glasses. These changes may be attributed to nonlinear absorption of the fs laser beam that generates defects such as oxygen deficient centers and non-bridging oxygen hole centers^{15, 16}.

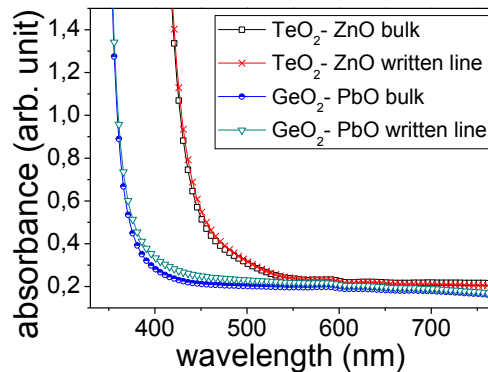


Figure 2. Absorption spectra of the samples (bulk and written area) in the TeO_2 -ZnO and GeO_2 -PbO glasses.

Figure 3(a) shows a schematic of the direction of the writing process. A picture captured of the output facet of the $\text{TeO}_2\text{-ZnO}$ glass waveguide after two single-line writing tests is shown in figure 3(b). It is possible to observe the damage at the air/glass interface, making an additional polishing step at the input and output facets necessary after laser processing. Figure 3(c) shows a double line waveguide composed of two writings separated from each other by $10\text{ }\mu\text{m}$, using a pulse energy of $30\text{ }\mu\text{J}$. Each dark line in Figure 3(c) corresponds to the border of a $6\text{ }\mu\text{m}$ wide region affected by the writing process. Guiding occurs in between the two centerlines.

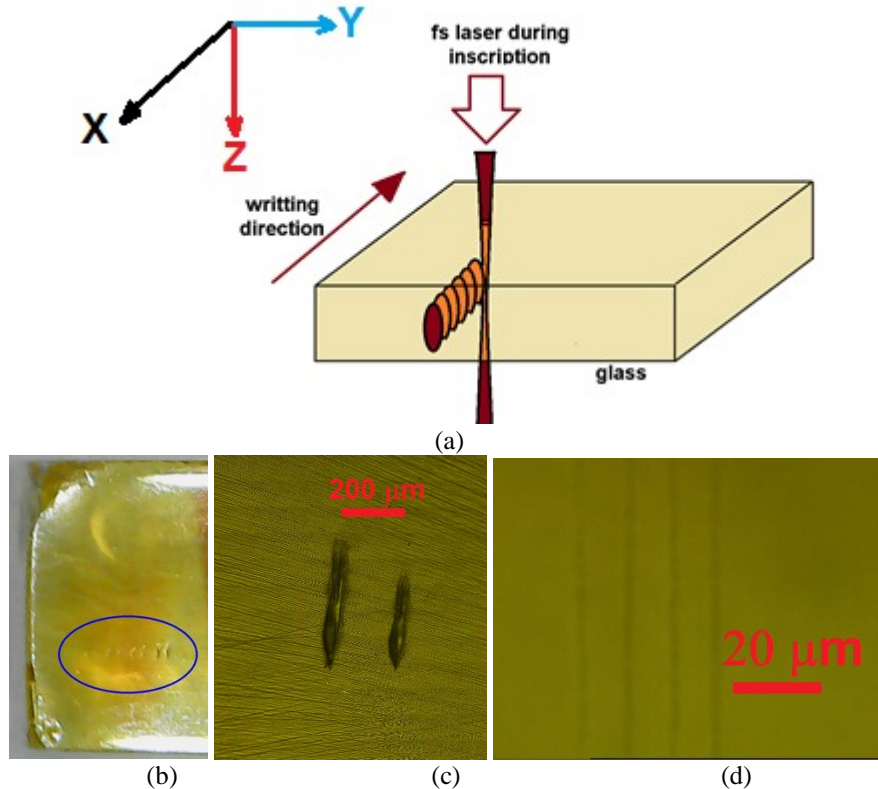


Figure 3(a) Schematic picture of the direction of the writing process. (b) Input/output interface of several writing tests of single lines in $\text{TeO}_2\text{-ZnO}$ glass. (c) Close up photo of the output facet of the $\text{TeO}_2\text{-ZnO}$ sample showing the effect of the fs laser writing at $30\text{ }\mu\text{J}$ (left) and $3\text{ }\mu\text{J}$ (right) laser pulse energy. (d) Top view microscope image of two written double line waveguides in the $\text{GeO}_2\text{-PbO}$ fabricated with $30\text{ }\mu\text{J}$ laser pulse energy.

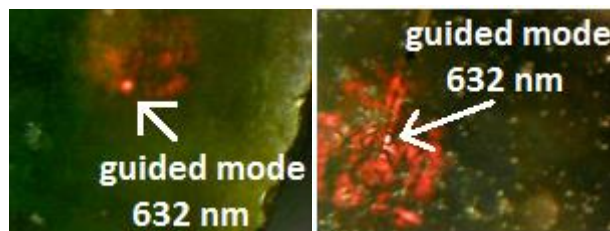


Figure 4. (a) and (b) images of the $\text{TeO}_2\text{-ZnO}$ and $\text{GeO}_2\text{-PbO}$ output faces respectively, showing waveguiding between the double lines for the two waveguides, $\text{TeO}_2\text{-ZnO}$ and $\text{GeO}_2\text{-PbO}$, written with $30\text{ }\mu\text{J}$, captured with a CCD at the waveguide exit facet.

To determine the optical losses using equation 1, a powermeter was used to measure the output power, P_2 and P_1 of the samples with total width of $Z_2=1.0$ cm, and a reduced width of $Z_1=0.6$ cm, respectively. The results are shown in table 3 where we can notice that the lowest optical losses were obtained for 30 μ J.

Table 3. Optical loss results for the samples written with different laser energies

Glass	Optical loss (dB/cm) Pulse energy = 30 μ J	Optical loss (dB/cm) Pulse energy = 3 μ J
TeO ₂ -ZnO	1.25	9.95
GeO ₂ -PbO	1.75	6.25

The near field profiles at the output of the waveguides are shown in figure 5. Comparing the results for TeO₂ – ZnO and GeO₂ – PbO glasses, varying writing speed and energy, we observe improvement of the near field profiles. Figure 5 shows the first obtained waveguide exit beams (writing speed: 6 mm/min, energy pulse=3 μ J). However, it was not possible to characterize those beams because of low confinement and high scattering of the signal. The other pictures are of lower loss waveguides obtained with writing speed of 1 mm/min and pulse energies of 3 and 30 μ J, respectively.

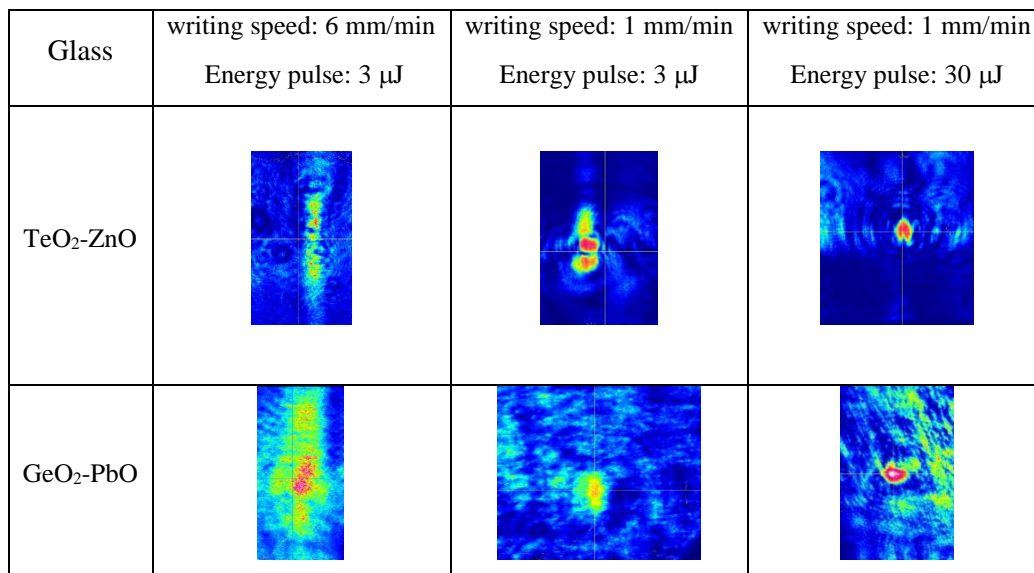


Figure 5. Near field mode profile (at 632 nm) of the beams transmitted by the waveguides.

The refractive index changes (Δn) were determined for the waveguides with the lowest optical losses, fabricated with 30 μ J of pulse energy and 1mm/min writing speed. At $\lambda=632$ nm we calculated $\Delta n = 1 \cdot 10^{-4}$ and $\Delta n = 8 \cdot 10^{-4}$ for the TeO₂ – ZnO and GeO₂ – PbO glasses, respectively.

A standard procedure was used to determine the M^2 of the output signal of the waveguides¹⁷, where the heights and widths of the transverse intensity distributions were measured at the $1/e^2$ -level to obtain beam propagation factors along perpendicular axes (horizontal x and vertical y). The obtained results are listed in table 4.

Table 4. M^2 measurements

Glass	M_x^2	M_y^2
TeO ₂ -ZnO	4.62	6.04
GeO ₂ -PbO	7.24	6.82

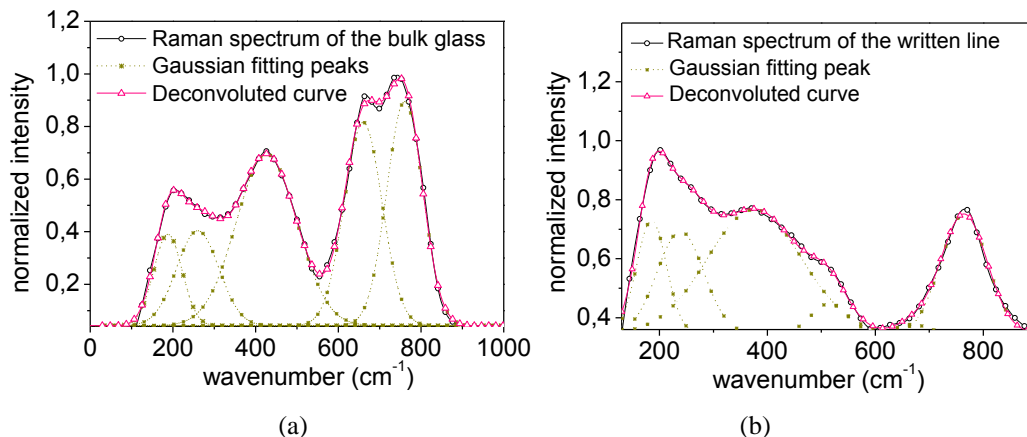
The Raman spectroscopy was crucial in the comprehension on how the fs laser affects the glassy network of the samples. The measurements in the focal region of the written line and between two written lines are shown in figure 6, where the spectra were deconvoluted into Gaussian peaks. In a first analysis we observed that the results in the region between the double lines are similar to the bulk glass, which indicates that no structural change is caused by the fs laser writing technique at the locus of waveguiding.

Some observations in the results of the $\text{TeO}_2 - \text{ZnO}$ are:

- The boson peak around 200 cm^{-1} (related to low frequency-vibrations and characteristic of amorphous materials) is the highest one in the fs laser written region (fig. 6(b)). Its amplitude is inversely proportional to the structural order of the sample¹⁸, which suggests the formation of different basic glassy units or a less connected structural glassy matrix.
- The peak at 250 cm^{-1} (related to ZnO_4 bending vibrations of Zn-O bonds in ZnO_4 tetrahedrons¹⁹) is the second highest in the fs laser written region (fig. 6(b)), a behavior not observed in the bulk glass, which suggest that the fs laser written affects the ZnO bonding vibrations of the glass modifier.
- The peak at 360 cm^{-1} (related to Te-O bonds of $-\alpha\text{TeO}_2$ ²⁰) is detectable only on the written region, which suggests changes in the network basic units relation. This peak is related to a stable crystalline phase, created by the laser writing process.
- The peak at 425 cm^{-1} is related to bending vibrations of Zn-O and Te-O-Te linkages formed by corner sharing of (TeO_4) , (TeO_{3+1}) polyhedrons and TeO_3 units and is visible in the bulk glass. In the written region this peak quenches and shifts to 450 cm^{-1} , which indicates that the writing processes leads to breaking of the bonds of Te-O-Te and Te -O- Zn²¹.
- The peak at 665 cm^{-1} , related to antisymmetrical TeO_4 vibrations that generally assumes large amplitudes in tellurite glasses²¹⁻²⁴, is not visible in the written region, which suggest that antisymmetrical vibrations of TeO_4 do not exist in the written region. This is another evidence of structural changes caused by the laser writing process.
- The peak at 745 cm^{-1} , related to pyramidal TeO_3 units, shifts to 763 cm^{-1} in the written region. This can be attributed to a lesser ordination of this kind of unit, which is a trigonal basic unit of tellurite glasses formed by broken bonds of Te-O²⁵.

Some observations for the results of the $\text{GeO}_2 - \text{PbO}$ Raman spectra are:

- A bigger similarity between the results of bulk and laser written areas is observed (figs 6(c) and 6(d)).
- The peak at 509 cm^{-1} , related to symmetric stretching vibrations along the Ge-O-Ge chain²⁶, shifts to 517 cm^{-1} in the written region. This can be related to a smaller density of these type of bonds in the written region.
- The other peaks at 610 , 780 and 900 cm^{-1} are similar for the bulk and the fs-written regions, indicating no influence of the laser writing process. These peaks are related to vibrations of Ge-O bonds in GeO_6 octahedral units and Ge-O- and GeO-Ge symmetric stretching, respectively.



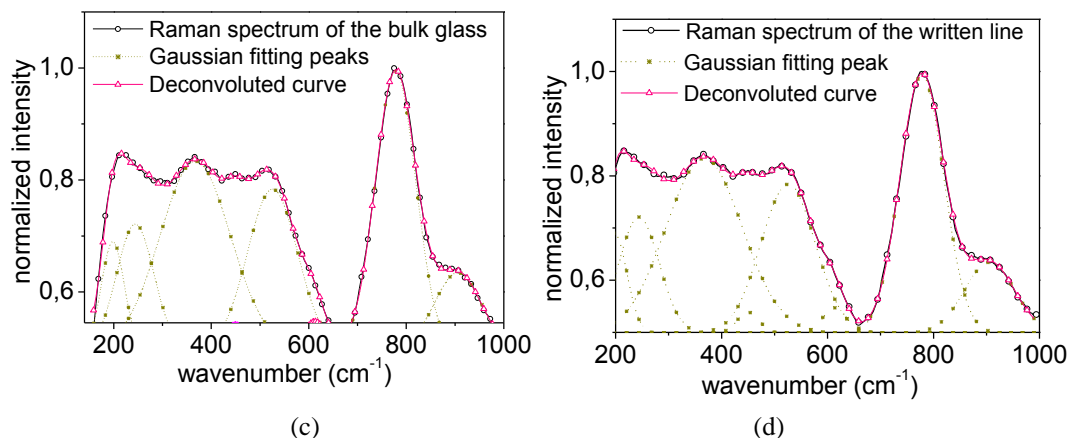


Figure 6. Deconvoluted Raman Spectra of TeO₂-ZnO glass: (a) Bulk area, (b) written area and deconvoluted Raman Spectra of GeO₂-PbO glass: (c) Bulk area, (d) written area.

Some works in the literature link structural aspects of similar glassy materials with the refractive index. N. Parveen et al demonstrated that in samples with glassy networks²⁷, formed by a mixture of TeO₄/TeO₃₊₁ and GeO₄ structural units, the increase of TeO₃₊₁/TeO₃ units leads to a decrease of the refractive index. A decrease in the TeO₄ content in the written region indicates a transformation of this basic unit into TeO₃, causing a refractive index modification, while the intermediate region between the two lines of writing keeps the bulk properties, having positive refractive index when compared to the adjacent written region.

For the GeO₂-PbO sample, the only evidences for structural modification are the Raman shift of the 509 cm⁻¹ peak (observed in the bulk) to 517 cm⁻¹ (observed in the written region) and the change of the transmittance window, as shown in figure 2.

It is important to notice that the thermo-mechanical effects caused by the laser irradiation in the fs regime are a complex event, and the conclusion about the phenomena caused by this laser irradiation depends strongly on the process parameters and materials evolved. A list of similar works that aggregate knowledge to this work is available in ²⁸.

In a next step it would be of interest to include doping into the glasses and measure gain²⁹. Also, for nonlinear optical devices, it would be of interest to experiment with heavy metal oxide glasses^{30,31}. Especially ytterbium and erbium co-doping is of interest there because well-known telecommunication applications^{32,33}.

4. CONCLUSIONS

Double line waveguides have been written with fs laser irradiation for the first time in TeO₂ - ZnO and GeO₂ - PbO glasses. The mechanisms by which guiding is obtained have been related to structural changes in the glassy matrix, characterized by Raman spectroscopy. The main result caused by this structural modification is a negative index change in the center of the fs laser written lines that causes a relative positive index increase between the two lines causing, thereby, the possibility of light guiding. The measured beam quality factors indicate low-order, multi-mode guiding and the losses of the waveguides are between 1-2 dB/cm.

ACKNOWLEDGEMENTS

We would like to thank CNPq (grant 307989 2013-5), CAPES and FAPESP (grant 2013 26113-6).

REFERENCES

- [1] Arms, M., Marshall, G. D., Dekker, P., Piper, J. A and Withford, M. J., "Ultrafast laser written active devices," *Laser Photon. Rev.*, 3, 535-544 (2009).
- [2] Huang, H., Yang, M. L. and Liu, J., "Femtosecond fiber laser direct writing of optical waveguide in glasses," *Proc. Nanophotonics and Macrophotonics for Space Environments V, SPIE Optical Engineering + Applications* 8164, 81640B (2011).
- [3] Ayiriveetil, A., Sabapathy, T., Varma, G. S., Ramamurthy, U. and Asokan, S., "Structural and mechanical characterization on ultrafast laser written chalcogenide glass waveguides," *Opt. Mater. Express* 6(8), 2530-2536 (2016).
- [4] Florea, C. and Winick K. A., "Fabrication and Characterization of Photonic Devices Directly Written in Glass Using Femtosecond Laser Pulses," *J. Lightwave Technol.* 21(1), 246-253 (2003).
- [5] Homoelle, D., Wielandy, S. and Gaeta, A. L., "Infrared photosensitivity in silica glasses exposed to femtosecond laser pulses," *Opt. Lett.*, 24(18), 1311-1313 (1999).
- [6] Pavel, N., Salamu, G., Voicu, F., Jipa F., Zamfirescu, M., Dascalu, T., "Efficient laser emission in diode-pumped Nd:YAG buried waveguides realized by direct femtosecond-laser writing," *Laser Phys. Lett.*, 10, 095802 (2013).
- [7] Nandi, P., Jose, G., Jayakrishnan, C., Debbarma, S., Chalapathi, K., Alti, K., Harmadhikari, A. K., Mathur, D., "Femtosecond laser written channel waveguides in tellurite glass," *Opt. Lett.*, 14(25), 12145-12150 (2006).
- [8] Siebenmorgen, J., Calmano, T., Petermann, K. and Huber, G., "Highly efficient Yb:YAG channel waveguide laser written with a femtosecond-laser," *Opt. Exp.*, 18, 16035-16041 (2010).
- [9] Bin, Q., Yang D., Guo-Ping, D., Fang-Fang, L., Liang-Bi, S., Sheng-Zhi, S. and Jian-Rong, Q., "Femtosecond Laser-Written Waveguides in a Bismuth Germanate Single Crystal," *Chin. Phys. Lett.* 26(7), 070601-1-070601-3 (2009).
- [10] Zhang, Y. J., Zhang, G. D., Bai, C. L., Chen, R., Stoian, R. and Cheng, G. H., "Double line and tubular depressed cladding waveguides written by femtosecond laser irradiation in PTR glass," *Opt. Mat. Express* 7, 2626-2635 (2017).
- [11] Fletcher, L. B., Witcher, J. J., Reichman, W. B., Arai, A., Bovatsek J., Krol D. W., "Changes to the network structure of Er-Yb doped phosphate glass induced by femtosecond laser pulses," *J. Appl. Phys.* 106(8), 83107-1-83107-5(2009).
- [12] Sotillo, B., Chiappini, A., Bharadwaj, V., Ramos, W., Fernandez, T. T., Rampini, S., Ferrari, vM., Ramponi, R., Fernández P., Gholipour, B., Soci and C., Eato, M. S., "Raman spectroscopy of femtosecond laser written low propagation loss optical waveguides in Schott N-SF8 glass," *Opt. Mat.* 72, 626-631 (2017).
- [13] da Silva, D. M., Kassab, L. R. P., Olivero, M., Lemos, T. B. N., da Silva, D. V., Gomes, A. S. L., "Er³⁺ doped waveguide amplifiers written with femtosecond laser in germanate glasses," *Opt. Mater.* 33, 1902-1906 (2011).
- [14] Ghatak, A., Thyagarajan, K., [An Introduction to Fiber Optics], Cambridge University Press, (1998).
- [15] Asai, T., Shimotsuma, Y., Kurita, T., Murata, A., Kubota, S., Sakakura, M., Miura K., Brisset, F., Poumellec B., Lancry M., "Systematic Control of Structural Changes in GeO₂ Glass Induced by Femtosecond Laser Direct Writing," *J. Am. Ceram. Soc.* 98, 1471-1477 (2015).
- [16] Manikandan, N., Rysanyanskiy and A., Toulouse J., "Thermal and optical properties of TeO₂ – ZnO – BaO glasses," *J. Non. Cryst. Solids* 358, 947 (2012).
- [17] Feise, D., Blume, G., Dittrich, H., Kaspari C., Paschke, K., Erbert, G., "High-brightness 635 nm tapered diode lasers with optimized index guiding," *Proc. SPIE* 7583, 75830V-1-75830V-12 (2010).
- [18] Malinovsky, V. K., Sokolo, A. P., "The nature of boson peak in Raman scattering in glasses," *Solid-State Commun.* 57, 757-761 (1986).
- [19] He, F., He, Z., Xiel, J., Li, Y., "IR and Raman Spectra Properties of Bi₂O₃-ZnO-B₂O₃-BaO Quaternary Glass System," *American Journal of Analytical Chemistry* 5, 1142-1150 (2014).
- [20] Amaya, I. V. G., Zayas M. E., Rivera, J. A., Álvarez S. A. G., Heredia A. G., Limón, G. A., Morales R. L., Rincón J. M., "Spectroscopic Studies of the Behavior of Eu³⁺ on the Luminescence of Cadmium Tellurite Glasses," *Hindawi Publishing Corporation Journal of Spectroscopy*, 478329, 1-7 (2015).
- [21] Sreenivasulu, V., Upender, G., Mouli, M. C., Prasad, M., "Structural, thermal and optical properties of TeO₂-ZnO-CdO-BaO glasses doped with VO²⁺," *Spectrochim Acta A Mol. Biomol. Spectrosc.* 148, 215-222 (2015).
- [22] Fernandez, T. T., Eaton, S. M., Valle, G. D., Vazquez, R. M., Irannejad, M., Jose, G., Jha, A., Cerullo, G., Osellame, and R., Laporta, P., "Femtosecond laser written optical waveguide amplifier in phospho-tellurite glass," *Opt. Express* 18 (19), 20289-20297 (2010).

- [23] Chagraoui, A., Yakine, I., Tairi A., Moussaoui, A., Talbi, M. and Naji, M., "Glasses formation, characterization, and cristal-structure determination in the Bi₂O₃–Sb₂O₃–TeO₂ system prepared in an air," *J. Mater. Sci.*, 46, 5439-5446 (2011).
- [24] Yadav A. K. and Singh, P., "A review of structure of oxide glasses by Raman spectroscopy," *RSC Adv.*, 5, 67583-67609 (2015).
- [25] Dos Santos, F. A., "Geração de segundo harmônico em vidros telluritos TeO₂ – LiNbO₃" (Doctoral dissertation), <<http://hdl.handle.net/11449/102528>> (10 March 2017).
- [26] Lucacel, R. C., Marcus, C. and Ardelean, I., "FTIR and Raman spectroscopic studies of copper doped 2GeO₂-PbO-Ag₂O glasses," *J. Optoelectron. Adv. M.*, 9(3), 747-750 (2007).
- [27] Parveen N., Jali, V. M. and Patil, S. T., "Structure and optical properties of TeO₂ – GeO₂ glasses," *IJASEAT*, 3, 89-94 (2016).
- [28] da Silva, D. S., Wetter, N. U., Rossi, W., Kassab, L. R. P. and Samad, R. E., "Production and Characterization of femtosecond laser-written double line waveguides in heavy metal oxide glasses," *Opt. Mater.* 75, 267-273 (2018).
- [29] De Assumpção, T. A. A., Da Silva, D. M., Camilo, M. E., Kassab, L. R. P., Gomes, A. S. L., De Araújo, C. B. and Wetter, N. U., "Frequency upconversion properties of Tm³⁺ doped TeO₂-ZnO glasses containing silver nanoparticles," *J. Alloys Compd.* **536**, 504-506 SUPPL.1 (2012).
- [30] Kassab, L. R. P., Courrol, L. C., Morais, A. S., Mendes, C. M. S. P., Tatumi, S. H., Wetter, N. U., Gomes, L. and Salvador, V. L. R., "Spectroscopic properties of lead fluoroborate and heavy metal oxide glasses doped with Yb³⁺," *J. Non. Cryst. Solids* **304**, 233-237 (2002).
- [31] De Assumpção, T. A. A., Kassab, L. R. P., Gomes, A. S. L., De Araújo, C. B. and Wetter, N. U., "Influence of the heat treatment on the nucleation of silver nanoparticles in Tm³⁺ doped PbO-GeO₂ glasses," *Appl. Phys. B Lasers Opt.* **103**(1), 165-169 (2011).
- [32] Bomfim, F. A., Martinelli, J. R., Kassab, L. R. P., Wetter, N. U. and Neto, J. J., "Effect of the ytterbium concentration on the upconversion luminescence of Yb³⁺/Er³⁺ co-doped PbO-GeO₂-Ga₂O₃ glasses," *J. Non. Cryst. Solids* **354**, 4755-4759 (2008).
- [33] Kassab, L. R. P., Courrol, L. C., Morais, A. S., Tatumi, S. H., Wetter, N. U. and Gomes, L., "Spectroscopic properties of lead fluoroborate glasses codoped with Er³⁺ and Yb³⁺," *J. Opt. Soc. Am. B Opt. Phys.* **19**(12), 2921-2926 (2002).